A Piecewise Sine Waveguide for Terahertz Traveling Wave Tube

Luqi Zhang (691490049@qq.com)
Institute of Applied Electronics, China Academy of Engineering Physics
Yi Jiang
Institute of Applied Electronics, China Academy of Engineering Physics
Wenqiang Lei
Institute of Applied Electronics, China Academy of Engineering Physics
Peng Hu
Institute of Applied Electronics, China Academy of Engineering Physics
Xianfeng Tang
Department of Physics, Southwest Jiao Tong University
Guowu Ma
Institute of Applied Electronics, China Academy of Engineering Physics
Hongbin Chen
Institute of Applied Electronics, China Academy of Engineering Physics
Yanyu Wei
School of Electronic Science and Engineering, University of Electronic Science and Technology University of China

Research Article

Keywords:

Posted Date: February 3rd, 2022

DOI: https://doi.org/10.21203/rs.3.rs-1304705/v1

Abstract

In this paper, a piecewise sine waveguide (PWSWG) is proposed as the slow-wave structure (SWS) to develop high power terahertz travelling wave tube (TWT). The PWSWG evolves from a rectangular waveguide oscillating with the piecewise sine curve along its longitudinal direction. Through the analysis of slow wave characteristics and transmission properties, it can be found that the PWSWG SWS has the advantages of high interaction impedance and excellent electromagnetic transmission performance. Furthermore, the calculation results of beam-wave interaction show that the TWT based on PWSWG SWS can generate the radiated power of 251W at the typical frequency of 220GHz, corresponding to a gain of 37.01dB and an interaction efficiency of 6.8%. Compared with the conventional sine waveguide (SWG) TWTs, the PWSWG TWT has higher interaction efficiency and shorter saturation tube length. In conclusion, the PWSWG will be considered as the potential SWS for high power terahertz radiation sources.

Introduction

Terahertz (THz) and technology has a wide application prospect in high-speed wireless communication, high resolution synthetic aperture radar imaging, biomedical diagnosis and space science exploration [1–4]. The exploration of terahertz radiation is one of the most important research directions in this field [5]. Benefiting from the energy conversion mechanisms of electron beams and electromagnetic waves [6], vacuum electronic devices (VEDs) are well suited for generating high-power terahertz radiation. Of all the terahertz VEDs, THz TWT has the outstanding combined performances in bandwidth and power capacity [7]. Therefore, this device has irreplaceable application potential in terahertz electromagnetic system.

As the core component of THz TWT, the slow-wave structure (SWS) directly determines the device performance of this high power terahertz radiation source. Nowadays, many kinds of slow wave structures including folded waveguide [8–9], corrugated rectangular waveguide (CRWG) [10–11], double corrugated rectangular waveguide (DCRWG) [12], staggered double-gate structure [13–14] and so on, have been proposed to develop high power radiation source in terahertz band. However, with the increase of operating frequency, the large transmission loss and strong reflection of these slow-wave structures limit the output power and bandwidth of THz TWT. The sine waveguide (SWG) SWS, which possesses the excellent transmission performance due to its uniform cross-section and simple energy coupling structures, has been put forward to design the THz VEDs [15–16]. Nevertheless, the longitudinal electrical field intensity of SWG SWS is too weak, resulting in the low interaction impedance of this structure [17]. Some modified sine waveguides including the flat-roofed sine waveguide (FRSWG) and the sine shape ridge waveguide (SSRWG) have been presented to improve the interaction impedance [18–19], but they either destroy the uniform cross-section or make machining difficulty. Thus, how to combine large interaction impedance with excellent electromagnetic transmission performance in the THz SWS is an important and significant issue for developing the high-power THz TWT.

Different from the existing THz SWSs, a new idea is put forward to improve the electric field distribution and avoid the leap point simultaneously by constructing the piecewise sine boundary of the SWS. A distinctive piecewise sine waveguide, which can be considered as the potential SWS for high power terahertz radiation sources, is analyzed for the first time in this paper. And this paper is organized as follows: At first, we analyze the slow-wave characteristics of the PWSWG SWS and explain the physical principle of interaction impedance growth in second section. In third section, the beam wave interaction circuit is built up based on the PWSWG SWS and the transmission parameters are calculated by electromagnetic simulation. The beam wave interaction performance of G-band PWSWG TWT is predicted by utilizing 3D particle-in-cell (PIC) algorithms in fourth section. Lastly, the summary for this paper is given in fifth Section.

Slow Wave Characteristics

Figure 1 (a) shows the PSRWG SWS that evolves from the rectangular waveguide with wide side length a and narrow side length b, in which its two E-planes are simultaneously oscillated up and down along the longitudinal direction with an amplitude h and a period p. Meanwhile, the oscillating amplitude should not exceed half of the narrow side length of the rectangular waveguide. Under these conditions, the cross section of the PSRWG SWS can be kept uniform and a rectangular electron channel with the cross-sectional area of $a \times h_b$ can just be formed. As can be seen from Figure 1 (b), the oscillating curve in H-plane is a piecewise sine curve formed by inserting line segments into peaks and troughs of the sine curve. The length of line segment is w and the period of sine curve is p_0, respectively.

The Eigen-mode solver in 3D electromagnetic simulation software Ansoft HFSS is used to analyze the slow-wave characteristics of the PWSWG SWS [20]. In order to obtain broad matching in the frequency range of 210-240GHz, the dimensional parameters of PWSWG SWS are partly optimized through calculations and given as follows: a=770μm, p=460μm, h=180μm, h_b=140μm. For the PWSWG SWS, the length of line segment w is key structural parameter that affects its slow wave characteristics. And the influence of the line segment length on dispersion properties and interaction impedances have been analyzed by the simulation method, as shown in Fig. 2. Fig. 2 (a) shows that the normalized phase velocity decreases and the cold bandwidth becomes narrow as the line segment length w increases from 30 to 130μm. At the same time, it can be seen from Fig. 2 (b) that the interaction impedance values increases gradually with the increase of line segment length w. Considering the balance between bandwidth and output power of TWT, a compromise is made between dispersion characteristics and interaction impedance values in our design. So, the optimized value of the line segment length w is 80μm.

Using the structural parameters obtained from the above optimization, the Brillouin curve of the PWSWG SWS has been depicted in Fig. 3. In order to ensure the best synchronization around 220GHz, the electron beam voltage is selected to be 20.9kV. It can be noted from Fig. 3 that this SSRWG SWS has a main competitive mode (Mode-2) that can cause back-wave wave oscillation. Although the interaction

impedance at the cross point is about 0.15ohm, this oscillation risk must be considered during the actual device design [21].

Then, the slow wave characteristics of the PWSWG SWS between the PWSWG SWS, the SWG SWS and the FRSWG SWS have been compared as shown in Fig. 4. Three SWSs have almost the same structural parameters, as given in Table 1. It should be pointed that to obtain the maximum interaction impedance in the comparison, the flattened height h_c is optimized to be a quarter of the beam tunnel height h_b [22]. From Fig. 4, we find that PWSWG SWS has the flatter dispersion curve and the lower normalized phase velocity compared to the other two SWSs. According to the synchronization conditions, we can infer that PWSWG SWS has wider bandwidth and lower synchronization voltage [21]. At the same time, the interaction impedances of PWSWG SWS are significantly larger than those of the other two SWSs in the frequency range of 210-240GHz. In detail, the interaction impedance of the PWSWG SWS at 220GHz is about 46.7% and 16.6% larger than the SWG SWS and the FRSWG SWS, respectively.

Table 1
Structural parameters of the PWSWG SWS, the SWG SWS and the FRSWG SWS

Parameter	PWSWG SWS	SWG SWS	FRSWG SWS
Wide side length a	770μm	770μm	770μm
Oscillating amplitude h	180μm	180μm	180μm
Oscillating period p	460μm	460μm	460μm
Beam tunnel height h_b	140μm	140μm	140μm
Line segment length d	80μm	-	-
Flattened height h_c	-	-	35μm

To understand the physical mechanism of interaction impedance growth, we can analyze it by interaction impedance K_c expression (1). Here, P_w represents the transmission power flow on the axis, E_{zn} and β_n represents the amplitude of the longitudinal electrical field and the phase constant of nth spatial harmonic. For the three SWSs, the TWT operates on the first positive space harmonic (n = +1).

$$K_c = \frac{|E_{zn}|^2}{2\beta_n{}^2 P_w} \quad (1)$$

The longitudinal electrical fields E_z of three SWSs at the typical frequency of 220GHz have been calculated, as shown in Fig. 5. For the PWSWG SWS, the longitudinal electric field distribution can be improved effectively by adjusting the line segment length. Apparently, the longitudinal electrical field

amplitude of the PWSWG SWS is much larger than the other two SWSs in the beam wave interaction region. This is the most important factor for the improvement of interaction impedance. The interaction impedance growth in SWS means that the coupling strength between electromagnetic wave and electron beam will become stronger. As a result, we can speculate that the TWT based on PWSWG SWS may have higher interaction efficiency and better amplification performance.

Transmission Properties

As mentioned in the introduction, the transmission performance of the THz SWS has become one of the most important factors for the THz TWT. A novel interaction circuit model based on PWSWG SWS has been designed in CST-MWS [23], as shown in Fig. 6. The beam wave interaction circuit model comprises 30 periods of the PWSWG SWS, both 5 periods of tapered section and both 1 period of matching section. The tapered sections are the SWG, and the oscillating amplitude h of the tapered section is gradually increasing and decreasing linearly to keep the perfect input and termination matching. Especially, the match section, which is composed of a quarter period SWG and three-quarter period SSRWG connected at the peak position, is proposed to avoid the leap point as illustrated in the inset of Fig. 6. The material of this interaction circuit is set as oxygen-free copper with a conductivity of 2.2×10^7S m^{-1} by considering non ideal surface roughness of the metal walls [24].

The transmission properties of the interaction circuit have been analyzed by utilizing the time-transient solver in CST MWS. From Fig. 7, we can see that the transmission parameter $S_{21} > -2.62$dB and the reflection parameter $S_{11} < -22$dB are achieved over the whole active band. It can be found that the PWSWG interaction circuit has good impedance matching and low loss characteristics.

Beam-wave Interaction Performance

Subsequently, the physical process of beam wave interaction in G-band PWSWG TWT can be simulated by utilizing 3D PIC algorithms. Based on the structural parameters obtained by previous optimization, we have built up the PWSWG interaction circuit in the CST PS [25]. In the PIC simulation, a sheet electron beam with an operating voltage of 20.9kV and a current of 175mA is adopted in the middle of tunnel. The cross sectional area of the sheet electron beam is selected as $400\times100\mu m^2$, and a uniform longitudinal magnetic of 1.5Telsa is applied here to confine the electron beam in the rectangular beam channel. Besides, we apply a driven signal with an input power of 50mW. To achieve the saturation output power at the typical frequency of 220GHz, the period numbers of the PWSWG interaction circuit have been optimized to be 100 by a large number of simulations.

The typical PIC simulation results at 220GHz have been obtained by PIC simulation, just as shown in Fig. 8. Fig. 8 (a) shows that the saturation output power can reach 251W at the end of the PWSWG interaction circuit. From Fig. 8 (b), we can note that most electrons are slowed down and a few are accelerated. For this reason, the majorities of electrons lose their energy and are gradually transformed into high frequency electromagnetic field energy. As can be observed in the inset of Fig. 8 (b), the electron

beam bunching occurs at the end of beam-wave interaction circuit. This classical physical phenomenon usually occurs at the end of this TWT. It can be seen from Fig. 8 (c) that the output signal can reach stability after 1.25ns of beam-wave interaction. The amplitude of the drive signal is amplified from 0.31622V to 22.4V, corresponding to a gain of 37.01dB. In addition, the frequency spectrum is concentrated at 220GHz and relatively pure as evident from the Fig. 8 (d). Since the termination is perfectly matched, the oscillation phenomenon is not observed. Nevertheless, an attenuator may be used to avoid the risk of oscillation in the practical device design [22]. To verify the amplitude-frequency response of the PWSWG TWT, we sweep the frequency point of the driven signal with the input power of 50mW. It can be seen in Fig. 9 that the 3dB bandwidth exceeds 40GHz with a maximum output power of 251W and an interaction efficiency of 6.8%.

Next, the SWG TWT and the FRSWG TWT with almost the same dimensional parameters as described previously have been built up in the CST PS. The synchronous voltages of these two TWTs are both about 21.5kV according as the synchronization condition. To obtain the maximum output power at 220GHz, the saturated period numbers of the SWG TWT and the FRSWG TWT have been optimized to be 120 and 102, respectively. The comparisons of the output power between the PWSWG TWT and the other two TWTs are given in the Fig. 10. The maximum output power of the PWSWG TWT at 220Hz is about 26.8% and 22.4% larger than the SWG TWT and the FRSWG TWT, respectively. Simultaneously, the PWSWG TWT possesses the wider bandwidth than the other two TWTs due to the flatter dispersion relation in the high frequency range.

From Fig. 11, we compare the interaction efficiency of the PWSWG TWT with the SWG TWT and the FRSWG TWT. The interaction efficiency of the PWSWG TWT is higher than the other two TWTs in the frequency range of 215-250GHz. Afterwards, we further compare the gains per unit length of the three TWTs, which can represent the amplifying performance of the SWS. As shown in Fig. 12, the gain per unit length of the PWSWG TWT exceeds 7.41dB/cm in the frequency range of 210-250GHz. It is evident that the gains per unit length of the PWSWG TWT are much higher than those of the other two TWTs over the whole operating band.

Summary

A distinctive piecewise sine waveguide (PWSWG) SWS, which can possess the advantages of both large interaction impedance and excellent electromagnetic transmission performance, is firstly reported in this paper. The simulation results indicate that the interaction impedance of PWSWG SWS has been increased due to the improvement of the longitudinal electrical field amplitude. Meanwhile, the design of match section for the PWSWG SWS is presented to inherit the excellent electromagnetic transmission properties from the SWG SWS. Moreover, the beam-wave interaction results predict that the PWSWG TWT has the larger radiated power, the higher interaction efficiency and more excellent amplifying performance than the conventional SWG TWTs. Therefore, this PWSWG should be considered as the promising SWS for the wide-band high power terahertz radiation source.

Declarations

Acknowledgements

This work was supported partly by the National Natural Science Foundation of China (Grant No.62101519), and in part by National Science Foundation of China (Grant No.12175217).

Author contributions

L.Q presented the idea, guided the research work and wrote the manuscript.Y. J and W.Q conducted the model design and HFSS simulations. P. H and X. F built up the CST simulation model and analyze the beam-wave interaction process. G.W., H. B. and Y.Y discussed the manuscript.

Competing interests

The authors declare no competing interests.

References

1. Sirtori, C. Bridge for the terahertz gap. *Nature***417**, 132 (2002). https://doi.org/10.1038/417132b
2. Siegel, P. H. Terahertz technology. *IEEE Trans. Microwave Theory Tech*. **50**,910 (2002).https://doi.org/10.1109/22.989974
3. Sherwin, M. Terahertz power. *Nature***420**,131(2002). https://doi.org/10.1038/420131a
4. Booske, J.H. et al.Vacuum electronic high power terahertz sources. *IEEE Trans. Terahertz Sci. Technol.***1**, 54 (2011). https://doi.org/10.1109/TTHZ.2011.2151610
5. Li,D. Z. et al.Terahertz Radiation from CombinedMetallic Slit Arrays. *Sci. Rep.* **9**,6804 (2019).https://doi.org/10.1038/s41598-019-43072-2
6. Dhillon, S. S., et al. The 2017 terahertz science and technology roadmap. *J. Phys. D: Appl. Phys.***50**, 043001 (2017). https://dx.doi.org/10.1088/1361-6463/50/4/043001
7. Bhattacharjee, S. et al. Folded waveguide traveling-wave tube sources for terahertz radiation. *IEEE Trans. Plasma Sci*.**32**, 1002 (2004).https://doi.org/10.1109/TPS.2004.828886
8. Joye, C. D. et al. Demonstration of a high power, wideband 220-GHz traveling wave amplifier fabricated by UV-LIGA.*IEEE Trans. Electron Devices*.**61**, 1672 (2014). https://doi.org/10.1109/TED.2014.2300014
9. Jiang, Y. et al. Demonstration of a 220-GHz continuous wave traveling wave tube. *IEEE Trans. ElectronDevices.* **68,** 3051 (2021). https://doi.org/10.1109/TED.2021.3075922
10. McVey, B. D. et al. Analysis of rectangular waveguide-gratings for amplifier applications.*IEEE Trans.Microw. Theory Tech.***42,** 995 (1994). https://doi.org/10.1109/22.293568
11. Xi, H.Z. et al. Continuous-wave Y-band planar BWO with wide tunable bandwidth. *Sci. Rep.* **8,** 348 (2018). https://doi.org/10.1038/s41598-017-18740-w

12. Mineo, M. et al. Improved corrugation cross-sectional shape in terahertz double corrugated waveguide.*IEEE Trans. Electron Devices***59,** 3116 (2012). https://doi.org/10.1109/TED.2012.2216534
13. Shin, Y. M. et al. Intense wideband terahertz amplification using phase shifted periodic electron-plasmon coupling.*Appl. Phys.Lett.***92**, 091501 (2008). https://doi.org/10.1063/1.2883951
14. Zhang, Z. et al. Multiple-beam and double-mode staggered double vane travelling wave tube with ultra-wide band. *Rep.* **10**, 20159 (2020).https://doi.org/10.1038/s41598-020-77204-w
15. Xu, X. et al. Sine Waveguide for 0.22-THz Traveling-Wave Tube.*IEEE Electron Device Lett.***32**,1152 (2011). https://doi.org/10.1109/LED.2011.2158060
16. Xu, X. et al. A watt-class 1-THz backward-wave oscillator based on sine waveguide.*Phys. Plasmas.***19**,013113 (2012). https://doi.org/10.1063/1.3677889
17. Zhang, L. Q. et al. Investigation of 0.38THz backward-wave oscillator based on slotted sine waveguide and pencil electron beam.*Phys. Plasmas***23**, 033111 (2016). https://doi.org/10.1063/1.4943410
18. Fang, S. Z. et al. Experimental verification of the low transmission loss of a flat-roofed sine waveguide slow-wave structure.*IEEE Electron Device Lett.***40**,808 (2019). https://doi.org/10.1109/LED.2019.2904080
19. Zhang, L. Q. et al. An ultra-broadband watt-level terahertz BWO based upon novel sine shape ridge waveguide.*J. Phys. D: Appl. Phys.***49**,235102 (2016).https://doi.org/10.1088/0022-3727/49/23/235102
20. Ansoft Corp. Ansoft HFSS User's Reference (Online) Available: http://www.ansoft.com.cn/
21. Yang, Q. et al. An optimal design of W-band truncated sine waveguide traveling wave tube. *Journal of Infrared and Millimeter Waves*.**37**,235 (2018). https://doi.org/10.11972/j.issn.1001-9014.2018.02.017
22. Gilmour, A. S. Klystrons, Traveling Wave Tubes, Magnetrons, Cross-Field Amplifiers, and Gyrotrons edited by Artech House (2011).
23. CST Corp. CST MWS Tutorials (Online) Available: http://www.cst.com/
24. Hou, Y. et al. A Novel Ridge-Vane-Loaded Folded-WaveguideSlow-Wave Structure for 0.22-THzTraveling-Wave Tube.*IEEE Trans. Electron Devices.* **60**, 1228 (2013). https:10.1109/TED.2013.2238941
25. CST Corp. CST PS Tutorials (Online) Available: http://www.cst.com/

Figures

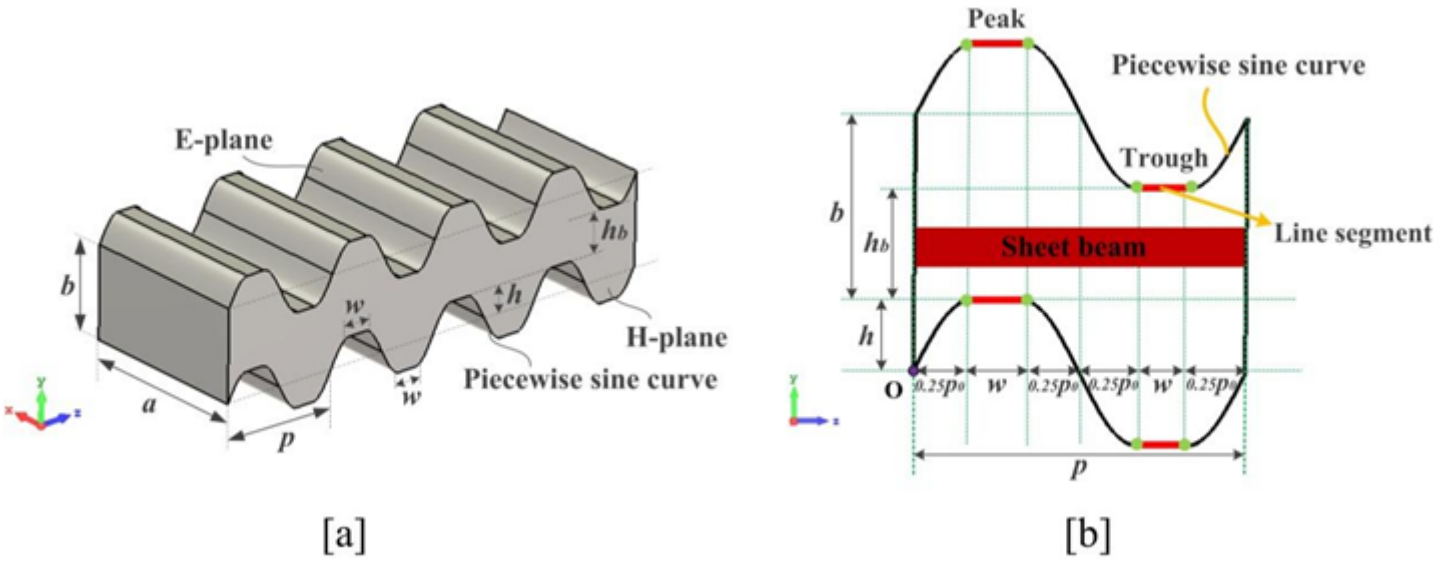

Figure 1

3-D structure model and dimensional parameters: (a) perspective view and (b) side view

Figure 2

Dispersion properties and interaction impedances of PSRWG SWS for the different *w* values

Figure 3

The Brillouin curve: the dash dot red line is the dispersion curve of the fundamental mode in the PWSWG SWS, the solid blue line is the electron-beam curve with a voltage 20.9kV

Figure 4

Comparisons of slow wave character is tics between the PWSWG SWS, the SWG SWS and the FRSWG SWS.

Figure 5

Longitudinal electrical field of the SSRWG SWS, the SWG SWS and the FRSWG SWS at 220GHz

Figure 6

Transmission model of the PWSWG interaction circuit in CST MWS. The inset gives the design of the matching section.

Figure 7

Transmission parameters and reflection parameters of the PWSWG interaction circuit

Figure 8

PIC simulation results at 220GHz. (a) Output power of the PWSWG interaction circuit as the function of the longitudinal distance. (b) The electron energy versus longitudinal distance. The inset shows the electron bunching at the end of interaction circuit. (c) Input and output signals. (d) Frequency spectrum of output signal.

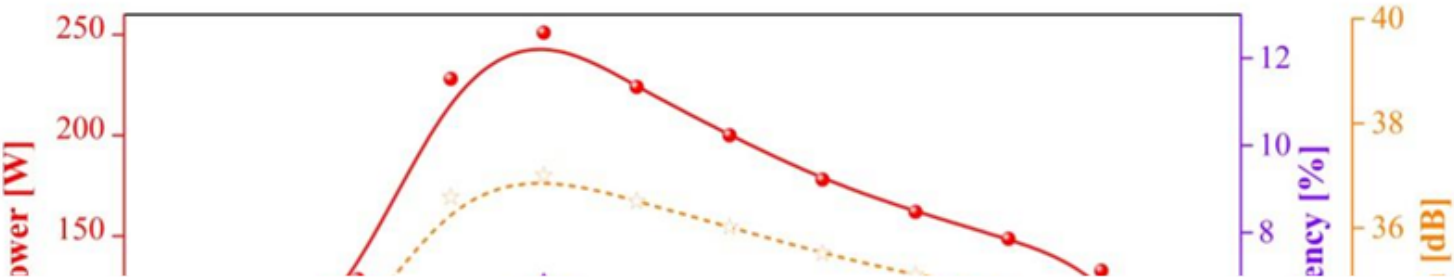

Figure 9

Output power, efficiency and gain of the PWSWG TWT versus frequency.

Figure 10

Comparisons of output powers of the PWSWG TWT, the SWG TWT and the FRSWG TWT

Figure 11

Comparisons of efficiencies of the PWSWG TWT, the SWG TWT and the FRSWG TWT.

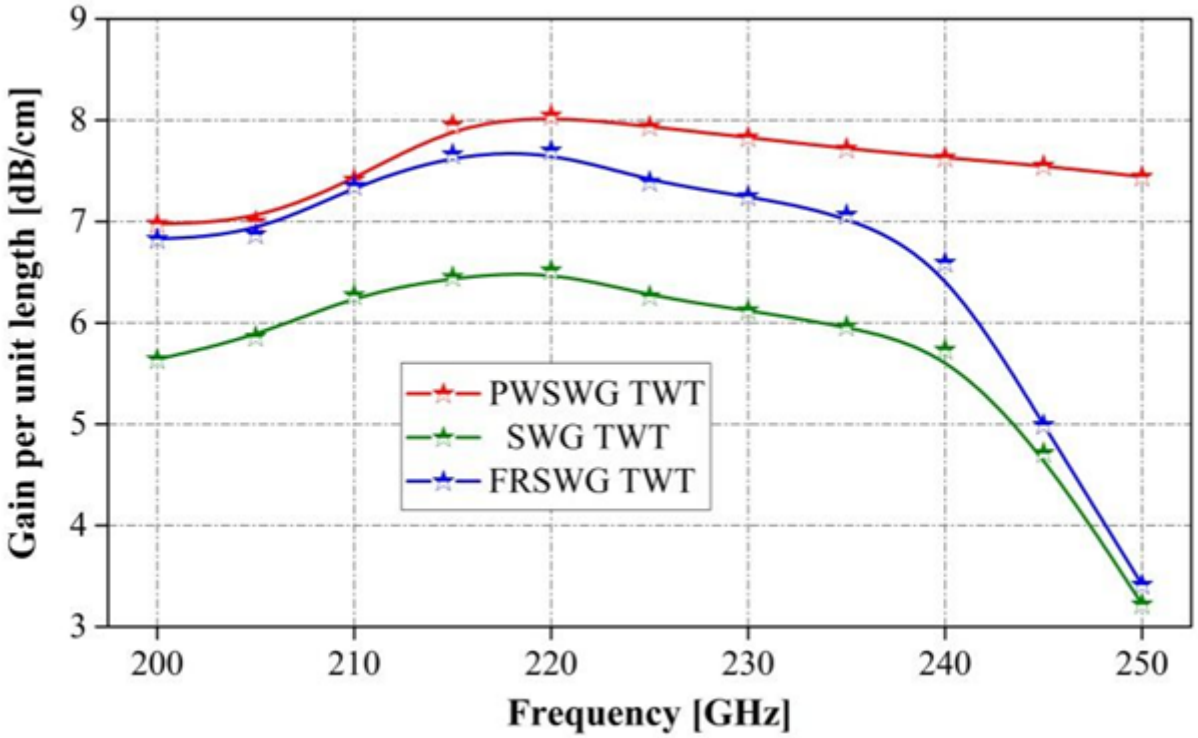

Figure 12

Comparisons of gains per unit length of the PWSWG TWT, the SWG TWT and the FRSWG TWT.